The Astrophysical Journal, 646:L49–L52, 2006 July 20

A NEW WATER VAPOR MEGAMASER

José Cernicharo and Juan R. Pardo
Departamento de Astrofísica Molecular e Infrarroja, Instituto de Estructura de la Materia, CSIC, Serrano 121, E-28006 Madrid, Spain; cerni@damir.iem.csic.es, pardo@damir.iem.csic.es

and

Axel Weiss
Max-Planck-Institut für Radioastronomie, Auf dem Hügel 69, D-53121 Bonn, Germany
Received 2006 April 10; accepted 2006 June 6; published 2006 July 12

ABSTRACT

We report on the detection of a new megamaser, the $3_{1,3}$–$2_{2,0}$ H_2O line ($\nu_0 = 183.310$ GHz) in Arp 220, using the Institut de Radioastronomie Millimétrique (IRAM) 30 m telescope. The line is about 350 km s^{-1} wide with a total luminosity of $\sim 2.5 \times 10^8$ K km s^{-1} pc^2. Although OH megamasers were first discovered in this source, no emission is seen in the $6_{1,6}$–$5_{2,3}$ H_2O transition ($\nu_0 = 22.235$ GHz), a line otherwise detected as a megamaser in about 50 sources to date. This fact puts interesting constraints on the physical conditions of the central region of Arp 220 that are further strengthened by the HCN and HNC $J = 3$–2 and $J = 1$–0 luminosities [in the range (1.5–10) $\times 10^8$ K km s^{-1} pc^2]. A scenario with $\sim 10^6$ star-forming cores similar to those found in Sgr B2 in the central kiloparsec of Arp 220 would be compatible with these data and would explain the lack of 22 GHz H_2O emission. This result opens up the possibility of using the 183 GHz H_2O line as an additional tool to explore the physical conditions in luminous and ultraluminous infrared galaxies (LIRGs and ULIRGs, respectively) and their starburst or active galactic nucleus (AGN) nature, with a potential interest for high angular resolution observations with the Atacama Large Millimeter Array (ALMA).

Subject headings: galaxies: individual (Arp 220) — galaxies: ISM — galaxies: starburst — ISM: abundances — radio lines: ISM

1. INTRODUCTION

Since the discovery of extragalactic water vapor maser emission by Churchwell et al. (1977) in M33 and the discovery of the first H_2O megamaser in NGC 4945 by Dos Santos & Lepine (1979), both of whom used the $6_{1,6}$–$5_{2,3}$ transition of this molecule ($\nu_0 = 22.236$ GHz), extensive research on these phenomena has been done, generally in parallel with OH maser and megamaser studies. OH megamasers were first discovered in Arp 220 by Baan et al. (1982). The most complete survey of 22 GHz H_2O megamasers published to date is by Braatz et al. (1997). Together with the still unpublished Kondratko et al. (2003) survey, and the recent additions reported in Braatz et al. (2004), Barvainis & Antonucci (2005), Sato et al. (2005), and Henkel et al. (2005), the number of detected sources exceeds 50.

H_2O and OH megamasers arise from galaxies with enhanced core activity, with a starburst or an AGN. Their luminosities are much higher than any Galactic maser counterpart. Their extragalactic nature make these masers very wide in velocity, generally several hundred kilometers per second. High angular resolutions, only accessible to interferometric observations, are necessary to reveal the regions responsible for the emission and to make progress in understanding the physical mechanisms leading to it.

Arp 220 is the nearest (at $z = 0.018$) prototype and is the best studied ULIRG. It is widely accepted that its large infrared luminosity ($1.4 \times 10^{12}\ L_\odot$; Soifer et al. 1987) is due to the fact that this object is a recent merger that has triggered a large starburst (see, e.g., the most recent continuum and OH megamaser interferometric maps by Rovilos et al. 2003, the VLA 43 GHz continuum and H53α maps by Rodríguez-Rico et al. 2005, or the high spatial resolution data at 3–25 μm by Soifer et al. 1999). In fact, recent VLBI observations by Lonsdale et al. (2006) have revealed up to 49 continuum sources, most probably radio supernovae that could have emerged from the large star formation activity in the nuclei of Arp 220.

Despite the presence of OH megamasers in Arp 220, no 22 GHz H_2O megamasers have been found in this source to date. Nevertheless, recent estimates of the H_2O column density toward the nucleus by González-Alfonso et al. (2004), using several far-IR H_2O lines seen in absorption by the *Infrared Space Observatory* (*ISO*) in the range 50–200 μm, give (2–10) $\times 10^{17}$ cm^{-2}.

In this Letter we report on the first detection of the $3_{1,3}$–$2_{2,0}$ line of H_2O ($\nu_0 = 183.310$ GHz) toward an ULIRG. A previous search by Combes et al. (1997) gave no detections. The first published detection of an extragalactic H_2O maser at 183 GHz has been done by Humphreys et al. (2005) toward NGC 3079, which is a local starburst galaxy at a distance of about 17 Mpc. Contrary to Arp 220, the 183 GHz water line in NGC 3079 appears as a narrow feature of width <40 km s^{-1}.

2. OBSERVATIONS AND RESULTS

Using the IRAM 30 m telescope, we observed the para-H_2O 3_{13}–2_{20}, HCN $J = 3$–2, and HNC $J = 3$–2 lines (ν_{rest} = 183.310, 265.886, and 271.981 GHz respectively) toward the center of Arp 220 ($\alpha_{2000} = 15^h34^m57^s.30$, $\delta_{2000} = 23°30'11''.4$). The observations were carried out under excellent weather conditions (zenith precipitable water vapor <1 mm) on 2004 March 18 and April 3 within the pooled observations. They were continued in 2005 January with even better weather conditions. We used the CD receiver setup with both 2 mm receivers tuned to 180.068 GHz (redshifted H_2O frequency) and the 1 mm receivers at 261.185 GHz (HCN) and 267.172 GHz (HNC), respectively. The system temperatures were ≈650 K at 2 mm and ≈400 K in the 1 mm band. The beam sizes of the 30 m telescope at 180 and 265 GHz are ≈14″ and ≈10″, respectively. The data were recorded using the 4 MHz filter banks (256

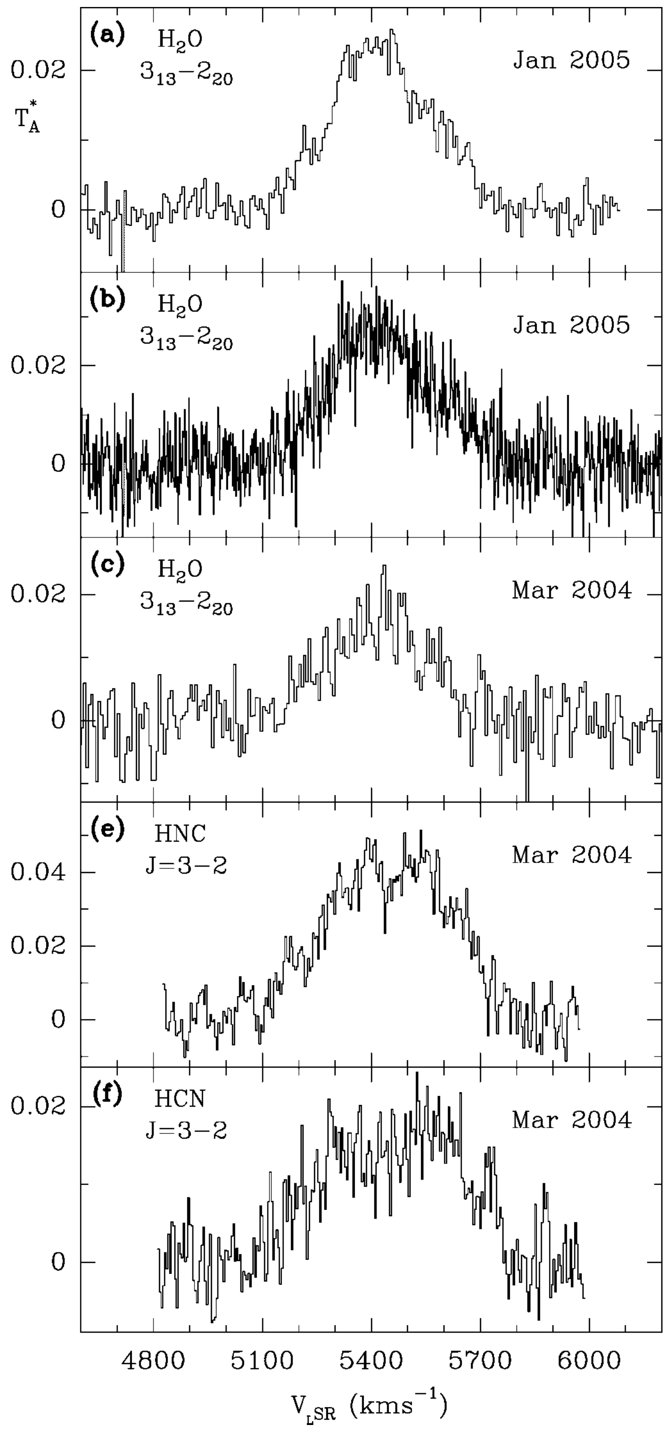

FIG. 1.—HCN (3–2), HNC (3–2), and H_2O 3_{13}–2_{20} lines observed with the IRAM 30 m telescope toward Arp 220. H_2O data obtained in two different runs are shown. Differences are probably related to calibration since the atmospheric conditions have a large impact on the atmospheric opacity at 180 GHz.

channels, 4 MHz resolution, 1 GHz bandwidth) on each receiver, leading to a channel spacing of 6.7 and 4.5 km s^{-1} in the 2 and 1 mm bands, respectively. In addition, the 1 MHz filter banks were connected to the 2 mm receivers (512 channels, 1 MHz or 1.7 km s^{-1} resolution, 500 MHz bandwidth).

The measurements were carried out in wobbler switching mode, with a switching frequency of 1 Hz and a wobbler throw of 90″ in azimuth. Pointing was checked on G34.3 and J1256−058 and was found to be stable within 3″. A calibration

TABLE 1
MEASURED LINE INTENSITIES ON ARP 220

Line	L (10^8 K km s^{-1} pc^2)	Ref.
H_2O $3_{1,3}$–$2_{2,0}$	2.5	1
HCN 1–0	6.4	2
	8.3	3
HCN 3–2	1.5	1
HNC 1–0	10.2	4
HNC 3–2	3.5	1

REFERENCES.—(1) This work; (2) Solomon et al. 1992; (3) Graciá-Carpio et al. 2006; (4) Hüttemeister et al. 1995.

scan was performed every 5 minutes using the standard hot/cold-load absorber scheme and using the ATM package (Cernicharo 1985; Pardo et al. 2001) for atmospheric corrections. A linear baseline was removed from each spectrum, and the final results are shown in Figure 1.

Compared to HCN and HNC $J = 3$–2, the $3_{1,3}$–$2_{2,0}$ H_2O line in Arp 220 has the same velocity extent (emission from ∼−200 to +250 km s^{-1}), although it is narrower at half-power (310 km s^{-1} compared to 410 km s^{-1} for HNC and 460 km s^{-1} for HCN according to Gaussian fits). The peak flux of the H_2O line is about 0.17 Jy or $T_{\rm MB}$ of about 35 mK (23 mK in T_A^* derived from a Gaussian fit). The HCN and HNC $J = 3$–2 observations are aimed at complementing previous observations of these molecules in the $J = 1$–0 transition. The flux uncertainty could be about 15% for the HCN and HNC observations, and it is larger for the H_2O data (probably ∼30%). Due to the better atmospheric conditions, we adopt the January observation for the discussions in this Letter.

3. DISCUSSION

According to Soifer et al. (1999), Arp 220 has two nuclei separated by about 1″, the strongest one has an average FWHM of about 0″.65 in the wavelength range 3–25 μm, and there is low-level extended emission (which probes the thermally emitting dust) at these wavelengths that extends beyond the two nuclei to cover about 2″–3″. The two nuclei have also been very well resolved in the radio continuum at 43 GHz with the Very Large Array (VLA) in Rodríguez-Rico et al. (2005). The separation has been determined to be 0″.9 ± 0″.1, and the two peaks lie at a position angle of 95°. The detected emission above 3 σ has an extension of approximately 1″.7 × 1″.4. Both nuclei have been similarly revealed at submillimeter wavelengths (using the continuum at 342 GHz and the CO 3–2 line at 345 GHz) by Wiedner et al. (2002), although extended CO emission is also present. The Arp 220 interferometric observations using HCN 1–0 by Radford et al. (1991) reveal a deconvolved source with a size between 2″ and 3″. Taking all these results into account, we will discuss the physical properties of the gas in the central region of Arp 220 (the central kiloparsec or so) that would explain our observations and some complementary data. For this task, we have calculated the corresponding luminosities of the observed para-H_2O $3_{1,3}$–$2_{2,0}$ line and the HCN and HNC $J = 3$–2 lines, and we have searched the literature for the luminosities of the corresponding $J = 1$–0 transitions of the latter two species. The values obtained are summarized in Table 1. For these estimates, we have considered a distance to Arp 220 of 72 Mpc, derived from its redshift of 5400 km s^{-1} and assuming a Hubble constant of 75 km s^{-1} Mpc^{-1}.

3.1. *The* 183 GHz H_2O *Emission*

Water vapor emission at 183 GHz arises from Galactic condensations in star-forming regions such as Orion (Cernicharo et al. 1994, 1999), Sgr B2 (Cernicharo et al. 2006), and other molecular clouds (Cernicharo et al. 1990, 1996; González-Alfonso et al. 1995). The para-H_2O 183 GHz line is rather easy to excite in most molecular clouds if the water column density is large enough (Cernicharo et al. 1994). Even for low densities, $n(H_2) = 10^4$–10^5 cm^{-3}, and low temperatures, $T_K \simeq 40$ K, the emissivity of this line could be higher than 100 K (see Cernicharo et al. 1994, 2006). This maser or suprathermal emission, depending on the density domain, has allowed for the detection of extended water emission before the *ISO* or the *Submillimeter Wave Astronomy Satellite* became available (Cernicharo et al. 1990, 1994). Model calculations for the 22, 183, and 325 GHz H_2O maser lines show that their intensities and the ratios between them change dramatically with the underlying physical conditions. Level inversion occurs easiest in the 183 GHz line, and its intrinsic brightness temperature can exceed a few thousand kelvins as, e.g., observed in Orion. In Figure 2 we show a set of large velocity gradient (LVG) models for these three lines covering kinetic temperatures from 40 to 300 K and H_2 densities from 10^3 to 10^9 cm^{-3}. From these plots, it is apparent that strong 183 GHz emission without detectable 22 GHz emission requires densities below $n(H_2) < 10^6$ cm^{-3} or fairly low temperatures (40 K). Detailed models of H_2O lines in Sgr B2 (Cernicharo et al. 2006) show that the strong 183 GHz emission line arises from gas at ∼40 K and $n(H_2) = 10^5$–10^6 cm^{-3}. Under these conditions, the 22 and 325 GHz lines would be extremely weak, which suggests that the gas giving rise to the observed 183 GHz intensity in Arp 220 may be similar to that seen in the Sgr B2 cores. This view is further supported by the far-IR H_2O lines seen in absorption toward the IR continuum in Arp 220 (Gonzalez-Alfonso et al. 2004), similar to the situation in Sgr B2. Simultaneous emission at 183 GHz and absorption in the far-IR H_2O lines can be understood by a layer of warmer gas (a few hundred kelvins), heated by nearby newly formed stars, surrounding the cooler cores (see Cernicharo et al. 2006 for details).

The detection of the 183 GHz H_2O line in Arp 220 suggests that in ULIRGs, this line, if present, should arise from regions spatially more extended than those responsible for the 22 GHz emission or the OH masers, as confirmed by the results shown in Lonsdale et al. (1998) and Rovilos et al. (2003). The observation of the 22, 183, and 325 GHz water lines should provide us with a quite complete picture of the water clouds around the central engines of these sources.

3.2. *The* HCN *and* HNC *Emission*

Our HCN and HNC (3–2) observations allow us to gain an independent test on the density of the dense gas in Arp 220. The ability of HCN lines to trace the dense, star-forming gas, which should be at least partly associated with the 183 GHz H_2O emission, has been shown in earlier studies (e.g., Solomon et al. 1992; Gao & Solomon 2004), although Graciá-Carpio et al. (2006) have raised some concerns about this tool in the $J = 1$–0 transition.

Contrary to most nearby galaxies, in Arp 220 the 3 mm emission of HNC is greater than that of HCN according to the results of Solomon et al. (1992) and Hüttemeister et al. (1995), a situation that in general is uncommon in AGNs or starburst galaxies according to Aalto et al. (2002). These latter authors found HNC $J = 1$–0 to be much weaker (even below the intensity of HCN $J = 1$–0) than the value published by Hüttemeister et al. (1995). However, our results using the $J = 3$–2 transition for both molecules support the HNC/HCN > 1 scenario. Because most studies have used only one transition (usually $J = 1$–0) to draw conclusions on the HNC/HCN ratio in LIRGs and ULIRGs, there has been a large debate among the different authors on the physical conditions that ultimately explain their own results. The use of different telescopes, with quite different calibrations, seems to add some confusion, and at the end the debate focuses on the adequateness of these tracers to probe high-density gas in ULIRGs. In this context, it is obviously helpful to use two different transitions for these molecules observed with the same telescope.

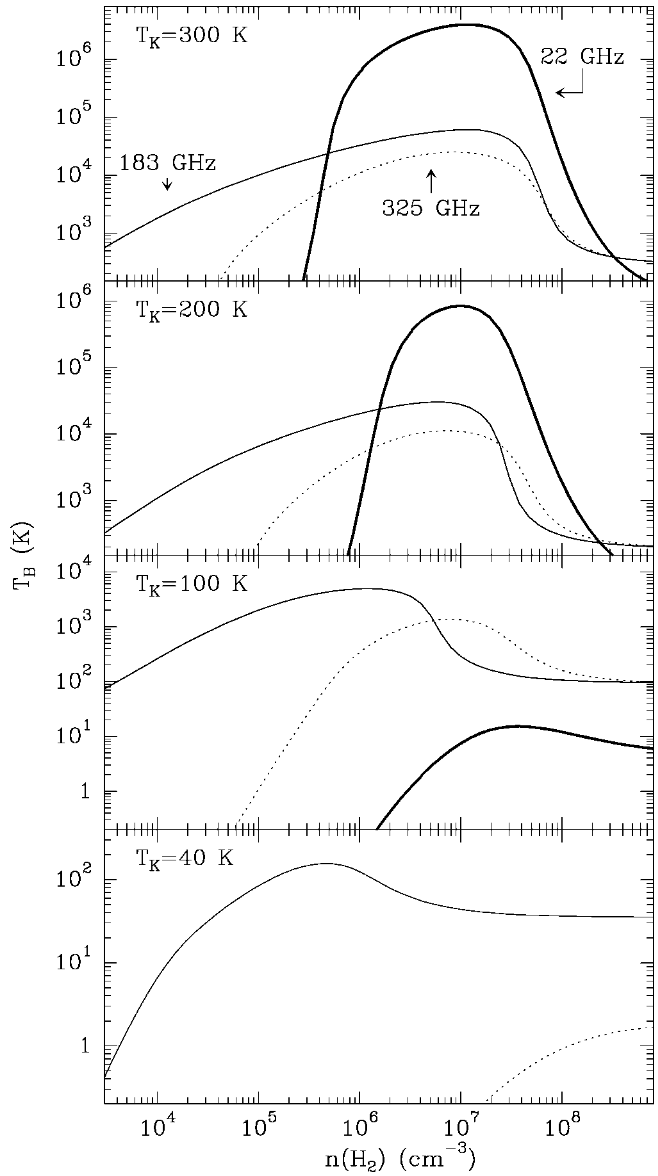

FIG. 2.—Comparison of the intensities of the 22, 183, and 325 GHz water masers in a wide range of physical conditions for a fixed N(p-H_2O)/Δv = N(o-H_2O)/Δv of 10^{18} cm^{-3} km s^{-1}.

Our observations show that the $J = 1$–0 line luminosity for both HCN and HNC are 3-4 times greater than those of $J = 3$–2. An LVG calculation indicates that for the dense part of the cores traced by the 183 GHz H_2O line in Sgr B2 (velocities of a few tens of kilometers per second, densities of 10^5–10^6 cm^{-3}, and $T_K \sim 40$ K), the brightness reached in the $J = 1$–0 transition of both HCN and HNC is between 1 and 10 K for column densities ranging from 10^{14} to 10^{15} cm^{-2}. In these conditions, the $J = 3$–2 transitions are about 3–4 times weaker. Changing the temperature and, more critically, the H_2 densities would quickly make the intensity ratios between the $J = 1$–0 and $J = 3$–2 transitions be in disagreement with the observations. This gives support to the scenario sketched in the previous section.

3.3. *Dense Cores in Arp 220*

In the assumption that a large starburst consisting of individual condensations similar to those in Sgr B2 is being traced by the H_2O 183 GHz maser emission detected in Arp 220, its magnitude can be estimated by comparison of the observed signals in both sources. In the 183 GHz observations toward Sgr B2 presented in Cernicharo et al. (2006), the line reaches a peak brightness of several tens of kelvins and widths of several tens of kilometers per second (an area of the order of 10^2–10^3 K km s^{-1}) toward the condensations Sgr B2(N) and Sgr B2(M). The size of these condensations traced by the H_2O 183 GHz maser emission is about 20″–30″, which means ∼1 pc for a distance to Sgr B2 of 8.5 kpc. The measured luminosity of the H_2O line in Arp 220, 2.5×10^8 K km s^{-1} pc^2, would translate into an average of ∼300 K km s^{-1} if we consider the emission restricted to the central kiloparsec of Arp 220. This means that Sgr B2–like condensations with a filling factor in that region of 0.2–1.0 (the latter value being possible due to projection effects) would be necessary to explain the observations, i.e., 2×10^5 to 10^6 sources in that central kiloparsec.

Concerning the absolute values of the HCN and HNC line intensities for Sgr B2–like cores given in the previous section, and taking again typical sizes of 1 pc, the observed intensity of these transitions in Arp 220 would also require of the order of 10^6 sources.

4. SUMMARY AND PROSPECTIVES

The detection of the $3_{1,3}$–$2_{2,0}$ line of H_2O with a luminosity of $\sim 2.5 \times 10^8$ K km s^{-1} pc^2 toward Arp 220 has been interpreted as being due to a starburst in the central kiloparsec or so, triggered by the merging nature of this object, with $\sim 10^6$ sources similar to the Galactic condensations Sgr B2(M) and Sgr B2(N). The luminosities of HCN and HNC in the $J = 1$–0 and $J = 3$–2 transitions further support this scenario.

The detection of the 183 GHz H_2O line in ULIRGs opens up several possibilities. First, the intensities of the 22 and 183 GHz H_2O lines could be an interesting tool for understanding the physical conditions in ultraluminous galaxies. Whereas the detection of 183 GHz H_2O emission and the nondetection at 22 GHz could imply an starburst scenario, the detection of very intense 22 GHz masers could be a sign of more extreme conditions, i.e., higher temperatures and densities in a spatially less extended region, typical of the AGN scenario. This idea deserves further research, for which the 325 GHz H_2O line, with intermediate-excitation conditions with respect to those of the 22 and 183 GHz ones, would serve as an extra constraint. Second, we point out that both the 183 and 325 GHz water lines will be observable with ALMA and that angular resolutions of ∼0″.1 could be achieved by taking into account the large brightness temperatures expected for the 183 GHz line at such angular scales.

This work has been supported by DGES and PNIE grants ESP2002-01627, AYA2002-10113-E, and AYA2003-02785-E.

REFERENCES

Aalto, S., Polatidis, A. G., Hüttemeister, S., & Curran, S. J. 2002, A&A, 381, 783
Baan, W. A., Wood, P. A. D., & Haschick, A. D. 1982, ApJ, 260, L49
Barvainis, R., & Antonucci, R. 2005, ApJ, 628, L89
Braatz, J. A., Henkel, C., Greenhill, L. J., Moran, J. M., & Wilson, A. S. 2004, ApJ, 617, L29
Braatz, J. A., Wilson, A. S., & Henkel, C. 1997, ApJS, 110, 321
Cernicharo, J. 1985, ATM: A Program to Compute Atmospheric Transmission between 0–1000 GHz, Internal Report of IRAM
Cernicharo, J., Bachiller, R., & Gonzalez-Alfonso, E. 1996, A&A, 305, L5
Cernicharo, J., Goicoechea, J. R., Pardo, J. R., & Asensio-Ramos, A. 2006, ApJ, 642, 940
Cernicharo, J., González-Alfonso, E., Alcolea, J., Bachiller, R., & John, D., 1994, ApJ, 432, L59
Cernicharo, J., Pardo, J. R., Gonzalez-Alfonso, E., Serabyn, E., Phillips, T. G., Benford, D., & Mehringer, D. 1999, ApJ, 520, L131
Cernicharo, J., Thum, C., Hein, H., John, D., Garcia, P., & Mattioco, F. 1990, A&A, 231, L15
Churchwell, E., Witzel, A., Pauliny-Toth, I., Sieber, W., Huchtmeier, W., & Roland, J. 1977, A&A, 54, 969
Combes, F., Nguyen-Q-Rieu, & Dinh-v-Trung, 1997, A&A, 323, 357
Dos Santos, P. M., & Lepine, J. R. D. 1979, Nature, 278, 34
Gao, Y., & Solomon, Ph. M. 2004, ApJS, 152, 63
González-Alfonso, E., Cernicharo, J., Bachiller, R., & Fuente, A. 1995, A&A, 293, L9
González-Alfonso, E., Smith, H. A., Fischer, J., & Cernicharo, J. 2004, ApJ, 613, 247
Graciá-Carpio, J., García-Burillo, S., Planesas, P., & Colina, L. 2006, ApJ, 640, L135
Henkel, C., Peck, A. B., Tarchi, A., Nagar, N. M., Braatz, J. A., Castangia, P., & Moscadelli, L. 2005, A&A, 436, 75
Hüttemeister, S., Henkel, C., Mauersberger, R., Brouillet, N., Wiklind, T., & Millar, T. J. 1995, A&A, 295, 571
Humphreys, E. M. L., Greenhill, L. J., Reid, M. J., Beuther, H., Moran, J. M., Gurwell, M., Wilner, D. J., & Kondratko, P. T. 2005, ApJ, 634, L133
Kondratko, P. T., Greenhill, L. J., Moran, J. M., Lovell, J. E. J., Jauncey, D. L., & Kuiper, T. B. 2003, AAS Meeting, 203, 63.09
Lonsdale, C. J., Diamond, P. J., Thrall, H., Smith, H. E., & Lonsdale, C. J. 2006, ApJ, in press (astro-ph/0604570)
Lonsdale, C. J., Lonsdale, C. J., Diamond, P. J., & Smith, H. E., 1998, ApJ, 493, L13 (erratum 494, L239)
Pardo, J. R., Cernicharo, J., & Serabyn, E. 2001, IEEE Antennas Propag., 49, 1683
Radford, S. J. E., et al. 1991, in Dynamics of Galaxies and Their Molecular Cloud Distributions, ed. F. Combes & F. Casoli (Dordrecht: Kluwer), 303
Rodríguez-Rico, C. A., Goss, W. M., Viallefond, F., Zhao, J.-H., Gómez, Y., & Anantharamiah, K. R. 2005, ApJ, 633, 198
Rovilos, E., Diamond, P. J., Lonsdale, C. J., Lonsdale, C. J., & Smith, H. E. 2003, MNRAS, 342, 373
Sato, N., Yamauchi, A., Ishihara, Y., Sorai, K., Kuno, N., Nakai, N., Balasubramanyam, R., & Hall, P. 2005, PASJ, 57, 587
Soifer, B. T., Neugebauer, G., Matthews, K., Becklin, E. E., Ressler, M., Werner, M. W., Weinberger, A. J., & Egami, E. 1999, ApJ, 513, 207
Soifer, B. T., Sanders, D. B., Madore, B. F., Neugebauer, G., Danielson, G. E., Elias, J. H., Lonsdale, C. J., & Rice, W. L. 1987, ApJ, 320, 238
Solomon, P. M., Downes, D., & Radford, S. J. E. 1992, ApJ, 387, L55
Wiedner, M., Wilson, C. D., Harrison, A., Hills, R. E., Lay, O. P., & Carlstrom, J. E. 2002, ApJ, 581, 229